

## Soft memory in a ferroelectric nanoparticle-doped liquid crystal

Rajratan Basu\*

*Department of Physics, Soft-matter and Nanomaterials Laboratory, The United States Naval Academy, Annapolis, Maryland 21402, USA*

(Received 25 November 2013; published 18 February 2014)

A small quantity of BaTiO<sub>3</sub> ferroelectric nanoparticles (FNP) was doped in a liquid crystal (LC), and the LC + FNP hybrid was found to exhibit a nonvolatile electromechanical memory effect in the isotropic phase. The permanent dipole moment of the FNPs causes the LC molecule to form short-range pseudonematic domains surrounding the FNPs. The FNP-induced short-range orders become more prominent in the isotropic phase when the global nematic order is absent. These short-range domains, being anisotropic in nature, interact with an external electric field, exhibiting a Fréedericksz-type transition. When the field is turned off, these domains stay oriented, showing a hysteresis effect due to the absence of any long-range order and restoring forces in the isotropic phase. The hysteresis graph for this memory effect shows a significant pretransitional behavior on approaching the nematic phase from the isotropic phase.

DOI: [10.1103/PhysRevE.89.022508](https://doi.org/10.1103/PhysRevE.89.022508)

PACS number(s): 61.30.Gd, 82.70.Kj

Memory effect in soft materials plays a crucial role in a wide range of physical properties and has drawn a great deal of research interest in fundamental and applied physics by exhibiting remarkable physical phenomena, such as a rewritable shape-memory effect in a semicrystalline poly( $\epsilon$ -caprolactone) [1], industrial applications of polymer-shaped memories in robotics [2], effect of soft memory in biocompatible devices [3], multilevel nonvolatile transistor memories in a star-shaped poly((4-diphenylamino)benzyl methacrylate) [4], and memory effects in soft polymer foams due to magnetoelectric coupling [5]. Liquid crystals (LCs), in particular, show fascinating memory effects, such as a binary optical memory effect in ferroelectric LCs [6], frustrated topological memory effects in nematic LCs [7], electric field driven bi-stable memory functions in dye-doped nematic LCs [8], and a surface-anisotropic-alignment memory effect in a nematic LC [9]. Recently, the long-range orientational order in LCs has been exploited very effectively to transfer order onto various nanoparticles [10–14]. Interestingly, it has been found to be a two-way street as the nanoparticles significantly improve some liquid crystalline properties. For examples, the presence of carbon nanotubes impacts favorably on the LC's electro-optic responses [15], quantum dots modify the chiral pitch in cholesteric LCs [16], and ferroelectric nanoparticles significantly enhance the orientational order and electro-optic response, reducing the threshold voltage [17–22]. In this paper, we describe a *nonvolatile electromechanical memory* effect at the nanoscale in a ferroelectric nanoparticle-doped LC. The memory effect is found in the isotropic phase and is detected through the dielectric hysteresis effect. This effect exhibits a significant pretransitional behavior on approaching the nematic phase from the isotropic phase and shows a linear dependency on the concentration of suspended ferroelectric nanoparticles.

BaTiO<sub>3</sub> ferroelectric nanoparticles (FNPs), obtained from U.S. Research Nanomaterials, Inc., had a diameter in the range of  $50 \pm 5$  nm. A small amount of the BaTiO<sub>3</sub> sample was first dispersed in acetone and was shaken on a vortex mixer for 8 h, followed by sonication for 5 h. This process reduces the

aggregation tendency of the FNPs. The liquid crystal 4-cyano-4'-pentylbiphenyl (5CB) then was added to the acetone + FNP mixture and was sonicated for 5 h, allowing the LC to dissolve completely into the solution. Finally, the acetone was evaporated at an elevated temperature, leaving a pure LC + FNP mixture. The process was repeated to produce several known concentrations of FNPs in the LC. Commercially manufactured LC cells (SA100A200uG180, planar rubbed from Instec Research Instrumentation Technology) with a 1° pretilt angle, 1 cm<sup>2</sup> semitransparent indium tin oxide coated area, and a  $d = 20$   $\mu$ m spacing were used for our experiments. The cells were filled with the pure LC or the LC + FNP mixtures at a temperature of  $T > 46$  °C in the isotropic phase by capillary action. The 5CB shows nematic to isotropic (NI) transition at  $T_{NI} = 35$  °C. Note that the small cell spacing tends to filter out any aggregates larger than  $d$ . Before performing any measurements, the FNP-doped LC cells were examined using a polarizing optical microscope. The optical micrographs revealed uniform nematic textures, such as that of the pure LC cell, indicating a uniform director field. There was no indication of phase separation or agglomerates at any temperature. Thus, at least on the length scales resolvable by visible light, the structure of the BaTiO<sub>3</sub> aggregates (if any) must be small enough that they do not perturb the director field due to their low concentration and uniform dispersion.

The nematic phase of an LC shows dielectric anisotropy  $\Delta\epsilon$  due to the anisotropic nature of the molecules where  $\epsilon_{\parallel}$  and  $\epsilon_{\perp}$  are the components parallel and perpendicular to the molecular long axis, respectively. For a positive dielectric anisotropic LC, such as 5CB,  $\epsilon_{\parallel} > \epsilon_{\perp}$ , and so, the *director field* (average direction of LC molecules) reorients parallel to an applied electric field. In a uniform homogeneously aligned parallel-plate cell configuration, the nematic director is initially aligned perpendicular to the applied electric field  $E$  due to the LC-substrate surface anchoring; but when the field magnitude is above a critical threshold, the director can reorient parallel to the applied field, obtaining a homeotropic configuration. This orientation process occurs because the nematic system is dielectrically anisotropic and experiences a torque proportional to  $\Delta\epsilon E^2$  [23]. The orientation process depends on the magnitude of the field and not on its sign. This is the essence of a Fréedericksz transition. When the field

\*basu@usna.edu

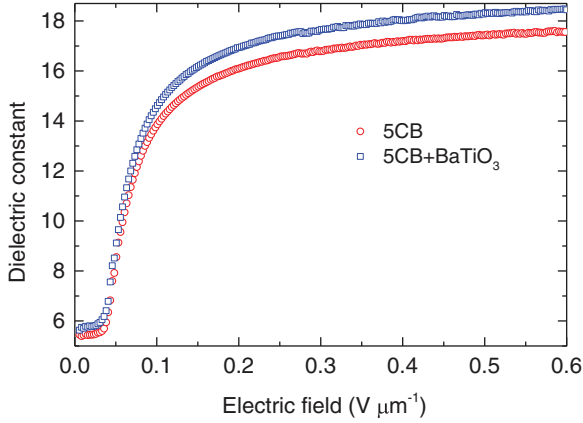


FIG. 1. (Color online) The dielectric constant as a function of applied rms field ( $f = 1000$  Hz) in the nematic phase ( $T = 25$  °C) for 5CB and 5CB + BaTiO<sub>3</sub> (0.525 wt %). This shows a typical Fréedericksz transition with a threshold field of  $0.03 \text{ V } \mu\text{m}^{-1}$ .

is turned off, the nematic director switches back the planar state due to the presence of the surface alignment process (i.e., anchoring energy) and its propagation into the bulk through nematic correlations. The isotropic phase, however, does not react to an electric field due to the absence of any orientational order. An automatic liquid crystal tester (Instec, Inc.) was used to measure the dielectric constant  $\epsilon$  of the cells as a function of an applied ac electric field at 1000 Hz both in the nematic and in the isotropic phases. The reason for applying the ac field is to avoid the effect of ion migration on the dielectric measurements.

Figure 1 shows a typical Fréedericksz transition in the nematic phase ( $T = 25$  °C) for 5CB and 5CB + FNP (0.525 wt %). The threshold field for both the samples is around  $0.03 \text{ V } \mu\text{m}^{-1}$ . As seen in Fig. 1, both the LC and the mixture undergo planar ( $\epsilon_{\perp}$ ) to homeotropic ( $\epsilon_{\parallel}$ ) orientational transition as the applied field increases. The dielectric anisotropy ( $\Delta\epsilon = \epsilon_{\parallel} - \epsilon_{\perp}$ ) for pure 5CB is  $\Delta\epsilon_{\text{LC}} = +12.1$  [24], whereas, the same for the composite system is found to be  $\Delta\epsilon_{\text{LC+FNP}} = +12.8$ . No hysteresis effect was observed on turning the field down to zero. Figure 2 shows the dielectric constant as a function of applied field in the isotropic phase ( $T = 42$  °C) for 5CB and 5CB + FNP (0.525 wt %). Pure 5CB shows a featureless behavior as expected. The hybrid system shows an increase in the dielectric constant above a threshold field  $E = 0.3 \text{ V } \mu\text{m}^{-1}$ , saturating at  $E = 1.4 \text{ V } \mu\text{m}^{-1}$ , exhibiting a Fréedericksz-like transition. The rate of change in the external field was  $\sim 2 \times 10^{-4} \text{ V } \mu\text{m}^{-1} \text{ s}^{-1}$ . The change in dielectric constant is  $\Delta\epsilon_{\text{LC+FNP}}^{\text{iso}} = 0.75$ . Note that  $\Delta\epsilon_{\text{LC+FNP}}^{\text{iso}} \approx \Delta\epsilon_{\text{LC+FNP}} - \Delta\epsilon_{\text{LC}}$ . This phenomenon depicts that the suspended FNPs induce a net orientational order in the LC system that responds to the external field in the isotropic phase. More interestingly, as Fig. 2 shows, the dielectric constant does not relax back to its original value on turning the field down to zero, manifesting a nonvolatile memory effect.

Spherical BaTiO<sub>3</sub> ferroelectric nanoparticles possess a spontaneous permanent polarization  $P = 0.26 \text{ C m}^{-2}$  [25]. Therefore, the local field due to this polarization around a

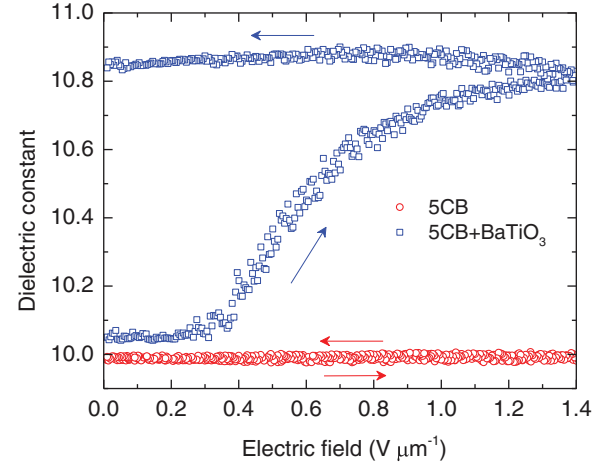


FIG. 2. (Color online) Dielectric constant as a function of the applied rms field ( $f = 1000$  Hz) in the isotropic phase ( $T = 42$  °C) for 5CB and 5CB + BaTiO<sub>3</sub> (0.525 wt %). The arrows show the field-cycle direction.

nanoparticle can be written as

$$\vec{E}_{\text{FNP}} = \frac{R^3 P}{3\epsilon_0 r^3} (2 \cos \theta \hat{r} + \sin \theta \hat{\theta}), \quad (1)$$

where the radius of the particle is  $R = 25 \text{ nm}$  and  $\epsilon_0$  is the free space permittivity. The average electric field magnitude at a distance of  $\xi = r - R = 5 \text{ nm}$  (i.e.,  $r = 30 \text{ nm}$ ) from the surface of the particle is  $\sim 10^{10} \text{ V m}^{-1}$ —this is four orders of magnitude higher than the maximum field applied across the LC cell (see Fig. 2). This local field, however, rapidly drops to  $\sim 10^7 \text{ V m}^{-1}$  at  $\xi = 200 \text{ nm}$  and to  $\sim 10^6 \text{ V m}^{-1}$  at  $\xi = 500 \text{ nm}$ . Consequently, the high field close to the FNPs can align an individual LC molecule over a distance  $\xi$  surrounding the particles. In the nematic phase, these short-range domains align with the global nematic director to reduce the free energy of the system. These local *pseudonematic domains* possess a different anisotropy than that of the bulk LC due to very strong fields from the suspended FNPs. These domains collectively increase the nematic orientational order, increasing the dielectric anisotropy of the system as shown in Fig. 1.

It has been calculated that [26] the dipole moment magnitude for a 5CB molecule is  $p = 6.5 \text{ D} = 2.15 \times 10^{-29} \text{ C m}$ . Thus, the energy  $U_{\text{FNP}} = -\vec{p} \cdot \vec{E}_{\text{FNP}} \sim -10^{-19} \text{ J}$  when the LC molecule aligns with the field close to the particle. The thermal energy in the isotropic phase at  $T = 45$  °C = 318 K is  $U_{\text{thermal}} \sim k_B T \sim 10^{-21} \text{ J}$ . Hence, the thermal energy is too small to eliminate the FNP-induced order in the isotropic phase. Due to the presence of these domains, the isotropic phase of 5CB + BaTiO<sub>3</sub> maintains a net anisotropy, exhibiting a Fréedericksz-like transition. Note that  $\Delta\epsilon_{\text{LC}} = +12.1$  and  $\Delta\epsilon_{\text{LC+FNP}}^{\text{iso}} = +0.75$ . So, roughly 6% of the LC molecules in the isotropic phase form the FNP-induced domains for the 0.525 wt % FNP concentration. If we assume, for simplicity, that the domains form spherical shells in the shape surrounding the spherical FNPs and the volume fraction of the LC that exhibits the net anisotropy in the isotropic phase is  $\Delta\epsilon_{\text{LC+FNP}}^{\text{iso}}/\Delta\epsilon_{\text{LC}}$ , then the shell thickness  $\xi$  would be  $\approx 50 \text{ nm}$ . From Eq. (1),

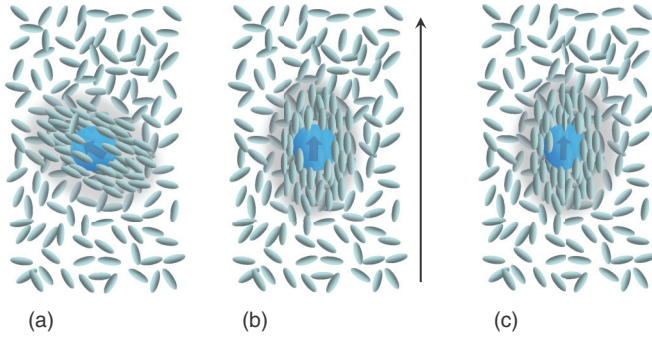


FIG. 3. (Color online) A schematic of the presence of a  $\text{BaTiO}_3$  FNP-induced pseudonematic domain in the isotropic phase. The sphere represents the FNP, the ellipsoids represent the LC molecules, and the shaded area represents the domain. (a) No electric field; (b) the electric field is turned on; (c) the electric field is turned off.

when  $\xi \approx 50$  nm (i.e.,  $r = 75$  nm),  $E_{\text{FNP}} \sim 10^9$  V m $^{-1}$ . Thus, to align all the LC molecules in the isotropic phase, one needs a field at least  $\sim 10^9$  V m $^{-1}$  across a capacitive-type cell—which is difficult to achieve without causing a dielectric breakdown.

The memory effect observed in Fig. 2 can be explained from the standpoint of the field-induced dynamic response of the nematic director. When an applied voltage across the cell is much higher than the threshold voltage, the nematic director undergoes a rotation to align along the applied field. As the field is turned off, the director relaxes back to the original orientation. The two characteristic times [27], rise (field on) and decay (field off), of the director can be described as

$$\tau_{\text{rise}} = \frac{\gamma_1 a^2}{\Delta \epsilon \epsilon_0 V^2 - K_{11} \pi^2}, \quad \tau_{\text{decay}} = \frac{\gamma_1 a^2}{K_{11} \pi^2}, \quad (2)$$

where  $\gamma_1$  is the rotational viscosity,  $a$  is the cell thickness,  $\epsilon_0$  is the free space permittivity,  $K_{11}$  is the splay elastic constant, and  $V$  is the applied voltage. Since  $\Delta \epsilon$  is zero in the isotropic phase for a pure LC, this phase does not interact with an external field, which can be understood from Eq. (2). The isotropic phase of  $5\text{CB} + \text{BaTiO}_3$  shows a nonzero anisotropy ( $\Delta \epsilon_{\text{LC+FNP}}^{\text{iso}} = 0.75$ ) due to the presence of the FNP-induced pseudonematic domains. However, as the global nematic order is absent, there is no long-range elastic interaction present in the isotropic phase, thus,  $K_{11} \approx 0$ . Clearly,  $\tau_{\text{rise}}$  gives a nonzero value using  $\Delta \epsilon_{\text{LC+FNP}}^{\text{iso}} = 0.75$  and  $K_{11} \approx 0$  (considering the domains do not interact with each other). But,  $\tau_{\text{decay}} \rightarrow \infty$  when  $K_{11} \approx 0$  in the isotropic phase. Therefore, when the field is turned off, the FNP-induced pseudonematic domains never come back to the original state as schematically shown in Fig. 3. In other words, when the field is off, there is no restoring force to mechanically torque these domains back into the original orientation in the isotropic phase, and the domains stay oriented (note that the backflow is negligible in a thin LC cell). This is the essence of a nonvolatile nanoelectromechanical memory effect as the electric field *mechanically* rotates the domains on the nanoscale. Note that short-range elastic interactions are present in the isotropic phase due to the presence of the pseudonematic domains. Also, some fraction of the FNP-induced nematic domains align parallel to the aligning substrates of the cells at the LC-substrate interfaces due to this short-range elastic

interaction. The observed threshold is perhaps an indication of surmounting these surface interactions.

From Eq. (2), in the isotropic phase,  $\tau_{\text{rise(LC+FNP)}}^{\text{iso}} = \gamma_1 / \Delta \epsilon_{\text{LC+FNP}}^{\text{iso}} \epsilon_0 E^2$ . After overcoming the local viscosity of the media, the pseudonematic domains start to reorient at  $E > 0.3$  V  $\mu\text{m}^{-1}$  (see Fig. 2), showing an apparent saturation at  $E = 1.4$  V  $\mu\text{m}^{-1}$ . Thus, it is a continuous reorientation process as  $E$  increases from  $0.3 \rightarrow 1.4$  V  $\mu\text{m}^{-1}$ . If the field is turned off at any intermediate stage between  $0.3$  and  $1.4$  V  $\mu\text{m}^{-1}$ , the domains will still be locked into that particular oriented state, showing an intermediate memory effect. Therefore, unlike bi-stable electronic memory devices, this nonvolatile nanoelectromechanical memory is a multistable memory function.

The FNP-induced pseudonematic domains are dielectrically anisotropic and experience a torque proportional to  $\Delta \epsilon_{\text{LC+FNP}}^{\text{iso}} E^2$ , similar to that of the nematic phase. So, as the domains do not respond to the sign of  $E$ , the memory cannot be erased by applying a positive or negative field. It is found that the field-induced reorientations of these anisotropic domains can only be erased by slowly cooling the system down to the nematic phase and then heating it up again to the isotropic phase. Therefore, this soft memory is rewritable after each temperature cycle: isotropic to nematic to isotropic.

It is observed that the critical phenomenon of phase transition in the LC greatly influences this memory effect. The amount of memory stored in a field cycle can be quantified by calculating the area under the hysteresis graph in Fig. 2. It is found that the hysteresis area changes significantly on approaching the nematic phase from the isotropic phase. After each field cycle at a given temperature in the isotropic phase, the hybrid was cooled down to the nematic phase ( $T = 25$  °C) at a rate of  $0.02$  °C/min to erase the memory. For consistency, each time before starting a new field cycle, the hybrid system was heated up from the nematic phase to the isotropic phase at  $T = 46$  °C at a rate of  $0.02$  °C/min and then was cooled down to the desired temperature in the isotropic phase at the same rate. Figure 4 shows the memory effect for  $5\text{CB} + \text{BaTiO}_3$  (0.525

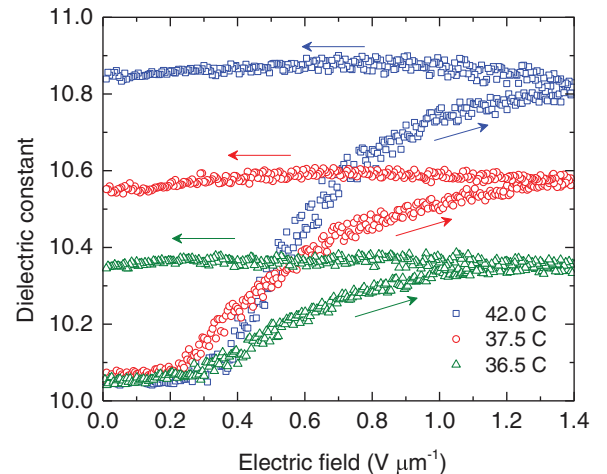


FIG. 4. (Color online) Dielectric hysteresis for  $5\text{CB} + \text{BaTiO}_3$  (0.525 wt %) at three different temperatures listed in the legend. The arrows show the field-cycle direction.

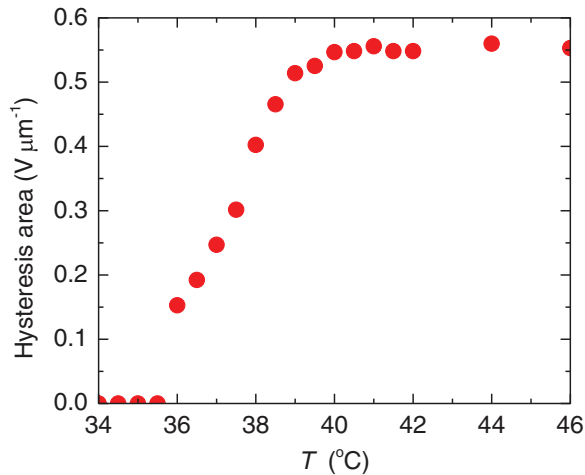


FIG. 5. (Color online) Dielectric hysteresis area for 5CB + BaTiO<sub>3</sub> (0.525 wt %) as a function of temperature. Note that  $T_{NI} = 35.5$  °C for 5CB + BaTiO<sub>3</sub> (0.525 wt %).

wt %) at three different temperatures in the isotropic phase. Figure 5 shows the hysteresis area as a function of temperature. Note that, for  $T \geq 40$  °C (i.e., deep in the isotropic phase), the hysteresis area stays almost constant, confirming that the small temperature change does not affect the domains orientations. On approaching the nematic phase, the hysteresis area gradually starts to decrease for  $T < 40$  °C, dropping 70% from its maximum value just before the transition at  $T = 36$  °C. The nematic fluctuation close to  $T_{NI}$ , perhaps, agitates the individual pseudonematic domains. This nematic fluctuation would enhance the overall elastic interaction, reducing the hysteresis effect. At a higher temperature, further away from  $T_{NI}$ , when this nematic fluctuation vanishes, the hysteresis reaches a constant value. After reaching the nematic phase at  $T < 35$  °C, the hybrid shows a typical Fréedericksz transition without any hysteresis effect.

This nonvolatile memory effect for three different FNP concentrations has been studied at  $T = 42$  °C and is plotted in Fig. 6. The memory effect decreases with decreasing FNP concentration as expected. The inset in Fig. 6 shows the hysteresis area as a function of FNP concentration. The linear behavior with a zero intercept confirms no memory effect for pure 5CB in the isotropic phase.

The dipolar interaction energy between a pair of FNPs is much larger than  $k_B T$ , so it is possible that the particles form chains. The chains may have a small contribution to the increase in the dielectric constant, but the effective hysteresis is due to the reorientation of the short-range nematic order. Note that the applied field has a frequency of 1000 Hz. Being embedded in the LC media, the FNPs (and the possible chains) would not be able to respond directly to this ac field. The pseudonematic domains, being dielectrically anisotropic, experience a torque proportional to  $\Delta\epsilon E^2$ . Thus, the domains respond to the magnitude of  $E$  and reorient as  $E$  increases.

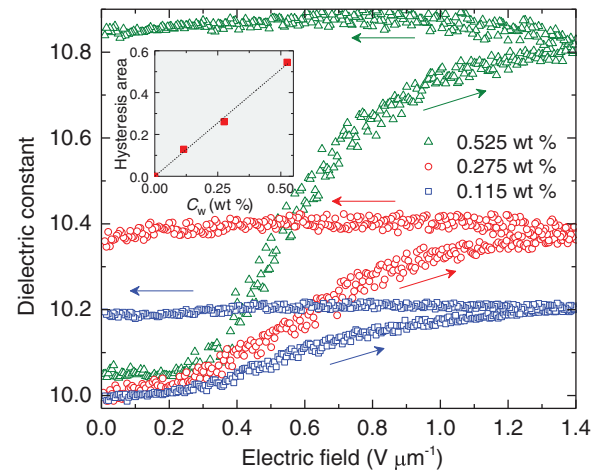


FIG. 6. (Color online) Dielectric hysteresis for 5CB + BaTiO<sub>3</sub> for three different concentrations listed in the legend. The arrows show the field-cycle direction. Inset: Hysteresis area ( $V \mu m^{-1}$ ) as a function of BaTiO<sub>3</sub> concentration in 5CB.

Since the domains are coupled to the FNPs, reorientation of the domains causes reorientation of the FNPs and not the other way around. Note that, when the field is turned off, it is the pseudonematic domains that do not relax back due to the absence of long-range elastic energy (hence, restoring force) in the isotropic phase, resulting in the observed hysteresis effect. The FNP chains (if any) do not play any important role here since no such hysteresis is observed in the nematic phase.

It is possible that some FNPs are present in aggregates in the LC, resulting in antiparallel-dipole arrangements. An antiparallel-dipole configuration can be approximately treated as a quadrupole, whose field magnitude drops as  $\sim 1/r^4$ . Thus, the field is still strong to form the pseudonematic domains close to the aggregates. However, as no aggregates were experimentally observed under an optical microscope, we conclude that, on the length scales resolvable by visible light, the structure of FNP aggregates (if any) must be small enough that they do not perturb the director field.

To summarize, we have demonstrated that, when a small quantity of BaTiO<sub>3</sub> ferroelectric nanoparticles is dispersed in 5CB LC, the hybrid in the isotropic phase exhibits an electromechanical memory effect which shows a significant pretransitional behavior on approaching the nematic phase from the isotropic phase. A simple model involving nonzero dielectric anisotropy and negligible elastic energy for the LC + FNP hybrid can explain the memory effect in the isotropic phase. The memory effect decreases with decreasing FNP concentration as the FNP-induced pseudonematic domains are responsible for the observed effect.

This work was supported by the Office of Naval Research under Award No. N001613WX20992 and the investment grant at the U.S. Naval Academy.

[1] M. Ebara, K. Uto, N. Idota, J. M. Hoffmana, and T. Aoyagi, *Soft Matter* **9**, 3074 (2013).

[2] A. Lendlein, A. M. Schmidt, and R. Langer, *Proc. Natl. Acad. Sci. USA* **98**, 842 (2001).

- [3] H.-J. Koo, J.-H. So, M. D. Dickey, and O. D. Velev, *Adv. Mater.* **23**, 3559 (2011).
- [4] Y.-C. Chiu, C.-L. Liu, W.-Y. Lee, Y. Chen, T. Kakuchi, and W.-C. Chen, *NPG Asia Mater.* **5**, e35 (2013).
- [5] L. Liu and P. Sharma, *Phys. Rev. E* **88**, 040601(R) (2013).
- [6] J. C. Curlander, R. A. Rice, and W. T. Cathey, *Appl. Opt.* **32**, 5759 (1993).
- [7] I. Mušević and S. Žumer, *Nature Mater.* **10**, 266 (2011).
- [8] J. K. Kim, K. Van Le, S. Dhara, F. Araoka, K. Ishikawa, and H. Takezoe, *J. Appl. Phys.* **107**, 123108 (2010).
- [9] A. B. Nych, D. Y. Reznikov, O. P. Boiko, V. G. Nazarenko, V. M. Pergamenschik, and P. Bos, *Europhys. Lett.* **81**, 16001 (2008).
- [10] M. D. Lynch and D. L. Patrick, *Nano Lett.* **2**, 1197 (2002).
- [11] I. Dierking, G. Scalia, and P. Morales, *J. Appl. Phys.* **97**, 044309 (2005).
- [12] R. Basu and G. Iannacchione, *Appl. Phys. Lett.* **93**, 183105 (2008).
- [13] I.-S. Baik, S. Y. Jeon, S. H. Lee, K. A. Park, S. H. Jeong, K. H. An, and Y. H. Lee, *Appl. Phys. Lett.* **87**, 263110 (2005).
- [14] R. Basu and G. S. Iannacchione, *Phys. Rev. E* **80**, 010701 (2009).
- [15] H.-Y. Chen, W. Lee, and N. A. Clark, *Appl. Phys. Lett.* **90**, 033510 (2007).
- [16] A. L. Rodarte, C. Gray, L. S. Hirst, and S. Ghosh, *Phys. Rev. B* **85**, 035430 (2012).
- [17] A. Rudzki, D. R. Evans, G. Cook, and W. Haase, *Appl. Opt.* **52**, E6 (2013).
- [18] A. N. Morozovska, M. D. Glinchuk, and E. A. Eliseev, *Phys. Rev. B* **76**, 014102 (2007).
- [19] M. Copic, A. Mertelj, O. Buchnev, and Y. Reznikov, *Phys. Rev. E* **76**, 011702 (2007).
- [20] L. M. Lopatina and J. V. Selinger, *Phys. Rev. Lett.* **102**, 197802 (2009).
- [21] F. Li, O. Buchnev, C. I. Cheon, A. Glushchenko, V. Reshetnyak, Y. Reznikov, T. J. Sluckin, and J. L. West, *Phys. Rev. Lett.* **97**, 147801 (2006).
- [22] Y. Reznikov, O. Buchnev, O. Tereshchenko, V. Reshetnyak, A. Glushchenko, and J. West, *Appl. Phys. Lett.* **82**, 1917 (2003).
- [23] P. G. De Gennes and J. Prost, in *The Physics of Liquid Crystals*, 2nd ed., edited by J. Birman, S. F. Edwards, C. H. Llewellyn Smith, and M. Rees, The International Series of Monographs on Physics Vol. 83 (Oxford University Press, New York, 1994).
- [24] D. A. Dunmur, M. R. Manterfield, W. H. Miller, and J. K. Dunleavy, *Mol. Cryst. Liq. Cryst.* **45**, 127 (1978).
- [25] B. Jaffe, W. R. Cook, Jr., and H. Jaffe, *Piezoelectric Ceramics* (Academic, New York, 1971).
- [26] C. J. Adam, S. J. Clark, G. J. Ackland, and J. Crain, *Phys. Rev. E* **55**, 5641 (1997).
- [27] E. Jakeman and E. P. Raynes, *Phys. Lett. A* **39**, 69 (1972).